

SCALING BEHAVIOR OF CIRCULAR COLLIDERS DOMINATED BY SYNCHROTRON RADIATION

Richard Talman*
 Laboratory for Elementary-Particle Physics Cornell University
 *richard.talman@cornell.edu

White Paper at the 2015 IAS Program on the Future of High Energy Physics

TUTORIAL LECTURE II

This file contains the material presented in lecture II. It mainly consists of pages extracted from the full paper, which has the title given above, with less important sections deleted and more important material underlined.

Scaling law 1: at fixed RF power, stored charge $\sim R^2$

Scaling law 2: luminosity depends on tunnel radius R and RF power P through their product $R \times P$

Scaling law 3: $\beta_y^{\max} \sim 1 / \beta^*_y$

Scaling law 4: luminosity $\sim \beta_y^{\max} / L^{*2}$

Universal upper limit: $\beta_y^{\max} / (D L_c) < 35 \text{ 1/m}$

$$\beta_y^{\max} \sim \frac{1}{\beta^*_y} \quad (a)$$

$$\text{luminosity} \sim \frac{\beta_y^{\max}}{L^{*2}} \quad (b)$$

$$\sim \frac{1}{\beta^*_y L^{*2}} \quad (c)$$

$$\text{(approx?) } \sim \frac{1}{L^*} \quad (d) \text{ YC}$$

CONTENTS

1 Introduction	3
1.1 Organization of the Paper	3
1.2 CepC, then CPPC in the Same Tunnel	3
1.3 Single Beam Parameters	4
1.4 Optimization Considerations	5
2 Ring Circumference and Two Rings vs One Ring	7
2.1 General Comments	7
2.2 Scaling up from LEP to Higgs Factory	8
Radius \times Power Scale Invariant.	8
Parameter Scaling with Radius.	8
2.3 Staged Optimization Cost Model.	8
2.4 Scaling of Higgs Factory Magnet Fabrication	9
2.5 Cost Optimization	10
2.6 Luminosity Limiting Phenomena	10
Saturated Tune Shift.	10
Beamstrahlung.	11
Reconciling the Luminosity Limits.	11
2.7 One Ring or Two Rings?	12
2.8 Predicted Luminosities	12
2.9 Reconciling the Luminosity Formulas	12
2.10 Qualitative Comments	15
2.11 Advantages of Vertical Injection and Bumper-Free, Kicker-Free, Top-Off Injection	16
3 Single Ring Multibunch Operation and Beam Separation	16
3.1 Electric Bump Beam (Pretzel) Separation	16
Operating Energies.	16
Bunch Separation at LEP.	17
Separated Beams and RF Cavities.	18
3.2 6 + 6 Element Closed Electric Bump	19
3.3 Bunch Separation Partition Number Shift	19
3.4 Beam Separation in Injection-Optimized Collider Lattice	19
4 Lattice Optimization for Top-Off Injection	20
4.1 Injection Strategy: Strong Focusing Injector, Weak Focusing Collider	20
Introduction.	20
4.2 Constant Dispersion Scaling with R	21
Linear Lattice Optics.	21
Scaling with R of Arc Sextupole Strengths and Dynamic Aperture.	22
4.3 Revising Injector and/or Collider Parameters for Improved Injection	22
Implications of Changing Lattices for Improved Injection.	22
5 $\mathcal{L} \times L^{*2}$ Luminosity \times Free Space Invariant	24
5.1 Estimating β_y^{\max} (and from it \mathcal{L})	24
Transverse Sensitivity Length.	25
Maximum β_y Phenomenology.	26
5.2 Turn-On Scenarios	27

6 APPENDICES	27
7 A. Synchrotron Radiation Preliminaries	27
8 B. Beamstrahlung	28
8.1 Determining Parameters to Suppress Beamstrahlung	28
8.2 Probability of Electron Loss Due to Beamstrahlung	30
8.3 Beamstrahlung from a Beam Bunch with Gaussian Longitudinal Profile	30
9 C. Simulation of Parameter Dependences of Tune Shift Saturation	31
10 D. Luminosity Formulas	32
10.1 Aspect Ratios and Hourglass Correction	32
10.2 RF-Power-Dominated Luminosity	33
10.3 Tune-Shift-Saturated Luminosity	33
10.4 Beamstrahlung-Limited Luminosity	36
10.5 Horizontal Beam Conditions	37

1 INTRODUCTION

1.1 Organization of the Paper

true for the p,p collider. But it already suggests that **the excess cost incurred in tunnel circumference needed for eventual p,p operation at energy approaching 100 TeV (over and above what could be minimally adequate for the Higgs factory) may not be exorbitant.**

the energy loss per turn, per electron, as a function of ring radius R , and electron beam energy E ;

$$U_1 \text{ [GeV]} = C_\gamma \frac{E^4}{R}, \quad (2)$$

where, for electrons, $C_\gamma = 0.8846 \times 10^{-4} \text{ m/GeV}^3$. For protons $C_\gamma = 0.7783 \times 10^{-17} \text{ m/GeV}^3$. For proton colliders preceding LHC synchrotron radiation (SR) was always negligibly small owing to the large proton mass. For the LHC, SR influenced the design only through the efforts needed to avoid dissipating the radiated energy at liquid Helium temperature. The post-LHC future circular collider will be the first for which beam dynamics and ring optimization will be dominated by SR. This has always been true for electron colliders.

There are three phenomena giving luminosity limits: \mathcal{L}^{RF} , *RF-power limitation*; \mathcal{L}^{bs} , *beamstrahlung limitation*; and \mathcal{L}^{bb} , *beam-beam interaction limitation*, all of which have complicated dependencies on ring parameters. **Since the achievable luminosity is equal to the smallest of these limits, the optimal choice of parameters requires them all to be equal.** To be specially exploited is a scaling law to be obtained according to which the optimized luminosity is a function only of the product RP^{RF} , tunnel-radius multiplied by RF power.

1.2 CepC, then CPPC in the Same Tunnel

The quite low Higgs particle mass makes a circular electron collider an effective Higgs factory. Furthermore, just as LHC followed LEP in the same tunnel, building first an electron collider, and later a proton collider in the same tunnel,

represents a natural future for elementary particle physics.

A possible modest initial cost increase can be far more than compensated by the improvement in ultimate proton collider performance.

The parameter most implicated in this discussion is, of course, the ring circumference. Once fixed this choice will constrain the facility for its entire, at least half century, life. Furthermore this choice needs to be made before any of the many remaining design decisions have to be made.

Minimizing the initial cost (and thereby improving the approval likelihood) makes optimizing the electron ring design more urgent than optimizing the proton ring design. In fact, since the ideal circumference for protons is surely greater than for electrons, **what is needed is to maximize the electron ring circumference while minimizing its cost—a seemingly impossible task.**

The thesis of this paper is that this optimization is not as hard as it seems. More concretely, it will be shown that making the electron ring circumference “unnecessarily large” (from the point of view of minimally adequate Higgs particle production) can increase its cost less than proportionally, if at all, provided the RF power is reduced proportionally. This argument relies on a scaling law according to which the optimized luminosity is a function only of the product of circumference times RF power.

$\beta_y^* = 0.008$ m, in order to establish trends. **According to the simulation model, the optimum is near $\beta_y^* \approx 5$ mm at the Higgs energy.** Numerical examples in the text are usually taken from the shaded rows.

Even in quite favorable cases the energy loss per turn U_1 is as much as several percent of the total energy. To keep the energy within 1% will then require a dozen or more RF accelerating sections. Because of its high energy loss, the Higgs factory will actually resemble a slowly curving linac. Nevertheless, it represents an economy, relative to a linear collider, to retain electrons along with most of their energy and restore their radiated energy every turn, rather than discarding and replacing them, as is required in a linear collider.

1.4 Optimization Considerations

This paper pays special attention to the beamstrahlung limitation pointed out by Telnov [3], and proceeds to quantify the limitation by a “beamstrahlung penalty” \mathcal{P}_{bs} . This penalty turns out to be so severe, and its onset (with increasing beam energy E) so sudden (see Figure 14) that a sensible strategy is to fix parameters so that \mathcal{P}_{bs} remains just barely consistent with the capability to replenish the lost particles.

In all cases the luminosity is limited by available RF power per beam. Following recent designs that have adopted $P_{rf} = 50$ MW as a kind of nominal choice, some tables in this paper use this value. **Other tables reflect my recommendation to reduce power to $P_{rf} = 25$ MW while doubling the ring circumference.** Fixing P_{rf} fixes the maximum total number N_{tot} of particles stored in each beam. At pre-LEP beam energies all other parameters would then have been adjusted to “saturate the beam-beam tune shift [4]”. At Higgs factory energies the RF power limitation, in conjunction with the beamstrahlung constraint, could make this impossible which will limit the luminosity accordingly.

E GeV	C km	R km	f KHz	U_1 GeV	eV_{excess} GeV	n_1 elec./MW	$U_1/(D/2)$ MV/m	$\delta = \alpha_4$	u_c GeV	ϵ_x nm	σ_x^{arc} mm
100	28	3.0	10.60	3.0	62	2.00e+11	0.626	0.0074	0.00074	6.354	0.523
150	28	3.0	10.60	14.9	50	3.94e+10	3.169	0.0249	0.00249	14.297	0.784
200	28	3.0	10.60	47.2	18	1.25e+10	10.016	0.0590	0.00591	25.417	1.05
250	28	3.0	10.60	115.2	-50	5.11e+09	24.453	0.1152	0.01155	39.715	1.31
300	28	3.0	10.60	239.0	-1.7e+02	2.46e+09	50.707	0.1991	0.01995	57.189	1.57
100	57	6.0	5.30	1.5	64	7.98e+11	0.157	0.0037	0.00037	3.177	0.37
150	57	6.0	5.30	7.5	58	1.58e+11	0.792	0.0124	0.00125	7.149	0.554
200	57	6.0	5.30	23.6	41	4.99e+10	2.504	0.0295	0.00296	12.709	0.739
250	57	6.0	5.30	57.6	7.4	2.04e+10	6.113	0.0576	0.00577	19.857	0.924
300	57	6.0	5.30	119.5	-54	9.85e+09	12.677	0.0996	0.00998	28.595	1.11
100	75	8.0	3.98	1.1	64	1.42e+12	0.088	0.0028	0.00028	2.383	0.32
150	75	8.0	3.98	5.6	59	2.80e+11	0.446	0.0093	0.00094	5.361	0.48
200	75	8.0	3.98	17.7	47	8.87e+10	1.409	0.0221	0.00222	9.532	0.64
250	75	8.0	3.98	43.2	22	3.63e+10	3.439	0.0432	0.00433	14.893	0.8
300	75	8.0	3.98	89.6	-25	1.75e+10	7.131	0.0747	0.00748	21.446	0.96
100	94	10.0	3.18	0.9	64	2.22e+12	0.056	0.0022	0.00022	1.906	0.286
150	94	10.0	3.18	4.5	61	4.38e+11	0.285	0.0075	0.00075	4.289	0.429
200	94	10.0	3.18	14.2	51	1.39e+11	0.901	0.0177	0.00177	7.625	0.573
250	94	10.0	3.18	34.6	30	5.68e+10	2.201	0.0346	0.00346	11.914	0.716
300	94	10.0	3.18	71.7	-6.7	2.74e+10	4.564	0.0597	0.00599	17.157	0.859
100	113	12.0	2.65	0.7	64	3.19e+12	0.039	0.0018	0.00018	1.589	0.261
150	113	12.0	2.65	3.7	61	6.31e+11	0.198	0.0062	0.00062	3.574	0.392
200	113	12.0	2.65	11.8	53	2.00e+11	0.626	0.0148	0.00148	6.354	0.523
250	113	12.0	2.65	28.8	36	8.17e+10	1.528	0.0288	0.00289	9.929	0.653
300	113	12.0	2.65	59.7	5.3	3.94e+10	3.169	0.0498	0.00499	14.297	0.784

Table 1: Ring parameters for rings of various bending radii, assuming 2/3 fill factor, with half of total straight section length D taken up by RF. The $U_1/(D/2)$ column therefore indicates the minimum required energy gain per meter to be supplied by the RF. u_c is the critical energy of the synchrotron radiation energy spectrum. α_4 is the appropriate damping decrement for $N^* = 4$ interaction points.

name	E GeV	C km	R km	f KHz	U_1 GeV	eV_{excess} GeV	n_1 elec./MW	$\delta = \alpha_2$	u_c GeV	ϵ_x^\dagger nm	σ_x^{arc} mm
Z	46	100	10.6	3.00	0.04	20	5.81e+13	0.00020	0.00002	0.573	2
W	80	100	10.6	3.00	0.34	20	6.08e+12	0.00107	0.00011	1.771	1.19
LEP	100	100	10.6	3.00	0.83	19	2.49e+12	0.00209	0.00021	2.767	0.972
H	120	100	10.6	3.00	1.73	18	1.20e+12	0.00361	0.00036	3.984	0.824
tt	175	100	10.6	3.00	7.83	12	2.66e+11	0.01119	0.00112	8.473	0.585

Table 2: Single beam parameters, assuming 100 km circumference. The second last column (\dagger) lists the value of ϵ_x appropriate only for $\beta_y^* = 5$ mm. Though determined by arc optics, ϵ_x has to be adjusted, according to the value of β_y^* , to optimize the beam shape at the IP. Other cases can be calculated from entries in other tables. U_1 is the energy loss per turn per particle. u_c is the critical energy for bending element synchrotron radiation. δ is the synchrotron radiation damping decrement.

Apart from its reduced cost compared to a linear collider (which is due to the surprisingly low mass the Higgs particle has been found to have) the greatest advantage of a circular collider is its well-understood behavior and correspondingly small risk.

2.1 General Comments

The quite low Higgs mass (125 GeV) makes a circular e+e- collider (FCC-ep) ideal for producing background-free Higgs particles. There is also ample physics motivation for planning for a next-generation proton-proton collider with center of mass energy approaching 100 TeV. This suggests a two-step plan: first build a circular e+e- Higgs factory; later replace it with a 100 TeV pp collider (or, at least, center of mass energy much greater than LHC). This paper is devoted almost entirely to the circular Higgs factory step, but keeping in mind the importance of preserving the p.p collider potential.

The main Higgs factory cost-driving parameter choices include: tunnel circumference C , whether there is to be one ring or two, what is the installed power, and what are the physics priorities. From the outset I confess my prejudice towards a single LEP-like ring, optimized for Higgs production at $E = 120$ Gev, with minimum initial cost, and highest possible eventual p.p energy.

2 RING CIRCUMFERENCE AND TWO RINGS VS ONE RING

Both Higgs factory power considerations and eventual p.p collider favor a tunnel of the largest possible radius R .

A good way to fix the circumference C is to simply extrapolate from earlier colliding beam rings as is done in Figure 2. Choosing $E = 300$ GeV to be the nominal beam energy yields circumference $C \approx 100$ km. Nothing in this paper is incompatible with this choice.

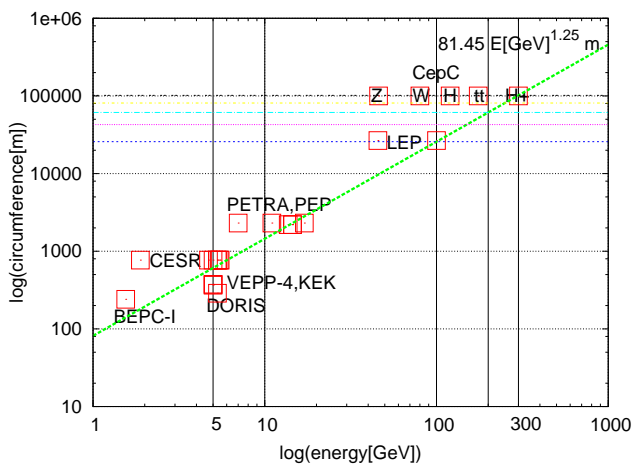


Figure 2: Relation between beam energy E and circumference C for numerous colliding beam rings.

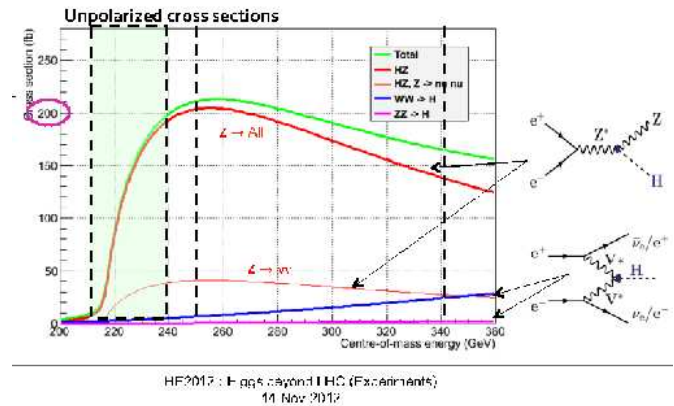


Figure 3: Higgs particle cross sections up to $\sqrt{s} = 0.3$ TeV (copied from Patrick Janot); $\mathcal{L} \geq 2 \times 10^{34} / \text{cm}^2 / \text{s}$, will produce 400 Higgs per day in this range.

2.2 Scaling up from LEP to Higgs Factory

Radius \times Power Scale Invariant. Most of the conclusions in this paper are based on scaling laws, either with respect to bending radius R or with respect to beam energy E . Scaling with bend radius R is equivalent to scaling with circumference C . (Because of limited “fill factor”, RF, straight sections, etc., $R \approx C/10$.)

Higgs production was just barely beyond the reach of LEP’s top energy, by the ratio $125 \text{ GeV}/105 \text{ GeV} = 1.19$. **This should make the extrapolation from LEP to Higgs factory quite reliable. In such an extrapolation it is increased radius more than increased beam energy that is mainly required.**

One can note that, for a ring three times the size of LEP, the ratio of E^4/R (synchrotron energy loss per turn) is $1.19^4/3 = 0.67$ —i.e. *less than final LEP operation*. Also, for a given RF power P_{rf} , **the maximum total number of stored particles is proportional to R^2 —doubling the ring radius cuts in half the energy loss per turn and doubles the time interval over which the loss occurs.** Expressed as a scaling law

$$n_1 = \text{number of stored electrons per MW} \propto R^2. \quad (3)$$

This is boxed to emphasize its fundamental importance. Following directly from Eq. (1), it is the main consideration favoring large circumference for both electron and radiation-dominated proton colliders.

There are three distinct upper limit constraints on the luminosity.

maximum luminosity results when the ring parameters have been optimized so the three constraints yield the same upper limit for the luminosity. For now we concentrate on just the simplest luminosity constraint $\mathcal{L}_{\text{pow}}^{\text{RF}}$, the maximum luminosity for given RF power P_{rf} . With n_1 being the number of stored particles per MW; f the revolution frequency; N_b the number of bunches, which is proportional to R ; σ_y^* the beam height at the collision point; and aspect ratio σ_x^*/σ_y^* fixed (at a large value such as 15);

$$\mathcal{L}_{\text{pow}}^{\text{RF}} \propto \frac{f}{N_b} \left(\frac{n_1 P_{\text{rf}} [\text{MW}]}{\sigma_y^*} \right)^2. \quad (4)$$

Consider variations for which

$$P_{\text{rf}} \propto \frac{1}{R}. \quad (5)$$

Dropping “constant” factors, the dependencies on R are, $N_b \propto R$, $f \propto 1/R$, and $n_1 \propto R^2$. With the $P_{\text{rf}} \propto 1/R$ scaling of Eq. (5), \mathcal{L} is independent of R . In other words, the

luminosity depends on R and P_{rf} only through their product RP_{rf} . Note though, that this scaling relation *does not* imply that $\mathcal{L} \propto P_{\text{rf}}^2$ at fixed R ; rather $\mathcal{L} \propto P_{\text{rf}}$.

In this paper this scaling law will be used in the form

$$\mathcal{L}(R, P_{\text{rf}}) = f(RP_{\text{rf}}), \quad (6)$$

assumes arcs are “benign”

the luminosity depends on R and P_{rf} as a function $f(RP_{\text{rf}})$ of only their product.

This radius/power scaling formula can be checked numerically by comparing Tables 6 and 8. The comparison is only approximate since other parameters and the scalings from LEP are not exactly the same in the two cases.

Parameter Scaling with Radius. For simplicity, even if it is not necessarily optimal, let us assume the Higgs factory arc optics can be scaled directly from LEP values, which are: phase advance per cell $\mu_x = \pi/2$, full cell length $L_c = 79 \text{ m}$. (The subscript “c” distinguishes the Higgs factory collider lattice cell length from injector lattice cell length L_i .)

Constant dispersion scaling formulas are given in Table 3. These formulas are derived in Section 4.2 “Lattice Optimization for Top-Off Injection”. They are then applied to extrapolate from LEP to find the lattice parameters for Higgs factories of (approximate) circumference 50 km and 100 km, shown in Table 5.

Parameter	Symbol	Proportionality	Scaling
phase advance per cell	μ		1
collider cell length	L_c		$R^{1/2}$
bend angle per cell	ϕ	$= L_c / R$	$R^{-1/2}$
quad strength ($1/f$)	q	$1/L_c$	$R^{-1/2}$
dispersion	D	ϕL_c	1
beta	β	L_c	$R^{1/2}$
tunes	Q_x, Q_y	R/β	$R^{1/2}$
Sands’s “curly H”	\mathcal{H}	$= D^2/\beta$	$R^{-1/2}$
partition numbers	$J_x/J_y/J_\epsilon$	$= 1/1/2$	1
horizontal emittance	ϵ_x	$\mathcal{H}/(J_x R)$	$R^{-3/2}$
fract. momentum spread	σ_δ	$\sqrt{\beta}$	$R^{-1/2}$
arc beam width-betatron	$\sigma_{x,\beta}$	$\sqrt{\beta\epsilon_x}$	$R^{-1/2}$
-synchrotron	$\sigma_{x,\text{synch}}$	$D\sigma_\delta$	$R^{-1/2}$
sextupole strength	S	q/D	$R^{-1/2}$
dynamic aperture	x^{max}	q/S	1
relative dyn. aperture	x^{max}/σ_x		$R^{1/2}$
pretzel amplitude	x_p	σ_x	$R^{-1/2}$

Table 3: *Constant dispersion Constant dispersion* scaling is the result of choosing cell length $L \propto R^{1/2}$. The entry “1” in the last column of the shaded “dispersion” row, indicates that the dispersion is independent of R when the cell length L_c varies proportional to \sqrt{R} with the phase advance per cell μ held constant.

2.4 Scaling of Higgs Factory Magnet Fabrication

Unlike the rest of the paper, this section is conjectural and idiosyncratic. It contains my opinions concerning how best to construct the Higgs factory room temperature magnets. It does not pretend to understand the economics of superconducting magnet technology. But it is also not ruled out that similar arguments and conclusions may be applicable to the eventual p,p collider.

As a disciple of Robert Wilson, one cannot avoid approaching the Higgs factory design challenge by imagining how he would have. **Certainly Bob Wilson would have endorsed Nima Arkani-Hamed's attitude that we strive for 100 TeV collisions "because the project is big", rather than "in spite of the fact the project is big".**

"How would Bob do it?" also suggests unconventional design approaches. At the early design stage, based on good, but limited, understanding of the task, one of his principles can be stated as "It is better for the tentative parameter choices to be easy to remember than to be accurate". In the current context he would certainly have liked the round numbers in a statement such as "To obtain 100 TeV collisions we need a ring with 100 km circumference", especially because of (or, possibly, in spite of) the fact that the CERN FCC group favors just these values.

Another Wilson attitude was that, if a competent physicist (where he had himself in mind) could conceptualize an elegant solution to a mechanical design problem, consistent with the laws of physics, then a competent engineer (where he again had himself in mind) could certainly successfully complete the design.

In extrapolating the room temperature magnet design from LEP to CepC one must first acquire a prejudice as to the vacuum chamber bore diameter. Many of the scaling formulas in this paper are devoted to determining this, along with other self-consistent parameters. To make the subsequent discussion as simple as possible one can accept, as a first iteration, the choice of making the magnet bore the same as LEP, promising to later improve this choice, in a second, or third, iteration, as necessary. It is my guess that the first iteration will be close.

In round numbers, the 100 km Higgs factory ring magnet length is four times as great as LEP's, and the Higgs factory energy is greater than the maximum LEP energy in the

ratio 120/100. The required Higgs factory magnetic field is therefore less than the LEP magnetic field in the ratio $1.2/4 = 0.3$. The stored magnetic energy density scales as the square of this ratio. With the magnetic bore constant, the Higgs factory stored magnetic energy is less than for LEP in the ratio $4 \times 0.3^2 = 0.36$. Ferromagnetic magnets are often costed in Joules per cubic meter. If this were valid the Higgs factory magnet would be three times cheaper than the LEP magnet.

When one actually looks into magnet costs one finds the calculation in the previous paragraph to be entirely misleading. The actual costs tend to be dominated by end effects, fabrication, transportation and installation. Accepting these costs as dominant would, one might think, force one to accept the Higgs factory magnet cost being proportional to tunnel circumference; this would be the cost of simply replicating LEP magnets. One reason this might be too conservative is that, with the Higgs factory cell length being longer, the magnets could be longer. But this would also be misleading since the LEP magnets were already as long as economically practical (because of fabrication, transportation and installation costs).

To hold down magnet costs, the inescapable conclusion to be drawn from this discussion is that the magnets have to be built *in situ*, in their final positions in the Higgs factory tunnel. This is the only possible way to prevent the magnet cost from scaling proportional to the tunnel circumference, or worse. (The same is probably true for superconducting magnets in the later p,p phase of the project.)

It is not at all challenging to build the Higgs factory collider magnets in place. With top-off injection these magnets do not have to ramp up in field. As a result they have no eddy currents and therefore do not need to be laminated.

Regrettably the same is not true for the injector magnet, which will be more challenging, and may be more expensive, than the collider magnet.

An even more quixotic argument for building the magnet in place is to compare the arcs of the collider to high voltage electrical power lines, which carry vast amounts of power over vast distances. For example a 10^6 V line, carrying 10^3 A, carries 10^9 W of power over a distance of 100 Km, with fractional energy loss of 1%. The arcs of the Higgs factory will similarly carry 10^{11} V at 10^{-2} A over a distance of 100 Km with fractional energy loss of 1%. Same power, same loss. One would not even think of building overland power lines in a factory before transporting them to where they are needed. The same should be true for accelerator magnets.

CPPC: For superconducting magnetic fields B in the range from 4 to 7 Tesla the cost per unit volume [16] is roughly proportional $B^{2/3}$ but increasing "more than linearly for higher magnetic fields", perhaps proportional to B at, say, 12 T. If true, at fixed bore diameter and fixed energy the magnet cost would be more or less independent of tunnel radius R , and there would be little need to worry about

the tunnel circumference being “too big” from this point of view.

As discussed previously the synchrotron radiation heat load cost is proportional to $1/R^2$ at fixed E . In principle, none of the synchrotron radiation has to be stopped at liquid helium temperature but, in practice, this is very hard to achieve. As with electrons, the reduced synchrotron radiation power load can be exploited to increase the stored beam charge by increasing R .

2.6 Luminosity Limiting Phenomena

Saturated Tune Shift. My electron/positron beam-beam simulation [4] dead reckons the saturation tune shift ξ_{\max} which is closely connected to the maximum luminosity. For an assumed $R \propto E^{5/4}$ tunnel circumference scaling, ξ_{\max} is plotted as a function of machine energy E in Figure 4. This plot assumes that the r.m.s. bunchlength σ_z is equal to β_y^* , the vertical beta function at the intersection point (IP).

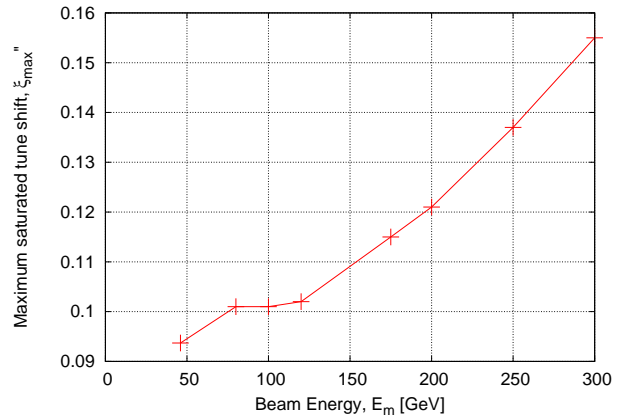


Figure 4: Plot of maximum tune shift ξ_{\max} as a function of maximum beam energy for rings such that $E \propto R^{5/4}$. The non-smoothness has to be blamed on statistical fluctuations in the Monte Carlo program calculation. The maximum achieved tune shift parameter 0.09 at 100 GeV at LEP was less than shown, but their torturous injection and energy ramping seriously constrained their operations.

Note that doubling the radius, while cutting the power in half, increases the cost only modestly, while leaving generous options for upgrading to maximize Higgs luminosity, as well as maximizing the potential p,p physics reach. The shaded row in Table 4 seems like the best deal.

The physics of the simulation assumes there is an equilibrium established between beam-beam heating versus radiation cooling of vertical betatron oscillations. Under ideal single beam conditions the beam height would be $\sigma_y \approx 0$.

This would give infinite luminosity in colliding beam operation—but this is unphysical. In fact beam-beam forces cause the beam height to grow into a new equilibrium with normal radiation damping. It is parametric modulation of the vertical beam-beam force by horizontal betatron and longitudinal synchrotron oscillation that modulates the vertical force and increases the beam height. The resonance driving strength for this class of resonance is proportional to $1/\sigma_y$ and would be infinite if $\sigma_y=0$ —*this too is unphysical.* Nature, “abhorring” both zero and infinity, plays off beam-beam emittance growth against radiation damping. However amplitude-dependent detuning limits the growth, so there is only vertical beam growth but no particle loss (at least from this mechanism). In equilibrium the beam height is proportional to the bunch charge. The simulation automatically accounts for whatever resonances are nearby.

Beamstrahlung. “Beamstrahlung” is the same as synchrotron radiation, except that it occurs when a particle in one beam is deflected by the electric and magnetic fields of the other beam. The emission of synchrotron x-rays is inevitable and the lost energy has to be paid for. Much worse is the occasional radiation of a single photon (or, by chance, the sum of two) of sufficiently high energy that the reduction in momentum causes the particle itself to be lost. This magnifies the energy loss by the ratio of the x-ray energy lost to the energy of the circulating electron by some two orders of magnitude. It is this process that makes beamstrahlung so damaging. It contributes directly to the so-called “interaction lifetime”. The damage is quantified by the beamstrahlung-dominated beam lifetime τ_{bs} .

The important parameter governing beamstrahlung is the “critical energy” u_c^* which is proportional to $1/\text{bunch-length } \sigma_z$; beamstrahlung particle loss increases exponentially with u_c^* . To decrease beamstrahlung by increasing σ_z also entails increasing β_y^* which reduces luminosity. A favorable compromise can be to increase charge per bunch along with β_y^* .

Reconciling the Luminosity Limits. The number of electrons per bunch N_p is itself fixed by the available RF power and the number of bunches N_b . For increasing the luminosity N_b needs to be *reduced*. To keep beamstrahlung acceptably small N_b needs to be *increased*. The maximum achievable luminosity is determined by this compromise between beamstrahlung and available power.

Three limiting luminosities can be defined: $\mathcal{L}_{\text{pow}}^{\text{RF}}$ is the RF power limited luminosity (introduced earlier to analyse constant luminosity scaling); $\mathcal{L}_{\text{sat}}^{\text{bb}}$ is the beam-beam saturated luminosity; $\mathcal{L}_{\text{trans}}^{\text{bs}}$ is the beamstrahlung-limited luminosity. Single beam dynamics gives $\sigma_y = 0$ which implies $\mathcal{L}_{\text{pow}}^{\text{RF}} = \infty$? Nonsense. Recalling the earlier discussion, the resonance driving force, being proportional to $1/\sigma_y$ would also be infinite. As a result the beam-beam force expands $\sigma_y = 0$ as necessary. *Saturation is automatic* (unless the single beam emittance is already too great for the beam-beam force to take control—it seems this condition was just barely satisfied in highest energy LEP operation [6]). For-

mulas for the luminosity limits are:

$$\mathcal{L}_{\text{pow}}^{\text{RF}} = \frac{1}{N_b} H(r_{yz}) \frac{1}{a_{xy}} \frac{f}{4\pi} \left(\frac{n_1 P_{\text{rf}} [\text{MW}]}{\sigma_y} \right)^2, \quad (11)$$

$$\mathcal{L}_{\text{sat}}^{\text{bb}} = N_{\text{tot}} H(r_{yz}) f \frac{\gamma}{2r_e} (\xi^{\text{sat}} / \beta_y), \quad (12)$$

$$\mathcal{L}_{\text{trans}}^{\text{bs}} = N_b H(r_{yz}) a_{xy} \sigma_z^2 f \left(\frac{\sqrt{\pi} 1.96 \times 10^5}{28.0 \text{ m } \sqrt{2/\pi}} \right)^2 \times \frac{1}{r_e^2 E^2} \left(\frac{91\eta}{\ln \left(\frac{1/\tau_{\text{bs}}}{f n_{\gamma,1} \mathcal{R}_{\text{unif}}^{\text{Gauss}}} \right)} \right)^2. \quad (13)$$

Here $H(r_{yz})$ is the hourglass reduction factor. If $\mathcal{L}_{\text{trans}}^{\text{bs}} < \mathcal{L}_{\text{sat}}^{\text{bb}}$ we must increase N_b . But $\mathcal{L}_{\text{trans}}^{\text{bs}} \propto N_b$, and $\mathcal{L}_{\text{pow}}^{\text{RF}} \propto 1/N_b$. We accept the compromise $N_{b,\text{new}}/N_{b,\text{old}} = \mathcal{L}_{\text{sat}}^{\text{bb}}/\mathcal{L}_{\text{trans}}^{\text{bs}}$ as good enough.

Parameter tables, scaled up from LEP, are given for 100 km circumference Higgs factories in Tables 6 and 8. The former of these tables assume the number of bunches N_b is unlimited. The latter table derates the luminosity under the assumption that N_b cannot exceed 200. Discussion of the one ring vs two rings issue can therefore be based on Table 8.

Some parameters not given in tables are: Optimistic=1.5 (a shameless excuse for actual optimization), $\eta_{\text{TelNov}}=0.01$ (lattice fractional energy acceptance), $\tau_{\text{bs}}=600$ s, $R_{\text{GauUnif}}=0.300$, $P_{r,f} = 25$ MW, Over Voltage=20 GeV, aspect ratio $a_{xy}=15$, $r_{yz} = \beta_y^*/\sigma_z=1$, and $\beta_{\text{arc max}}=198.2$ m.

With the exception of the final table, which is specific to the single ring option, the following tables apply equally to single ring or dual ring Higgs factories. The exception relates to N_b , the number of bunches in each beam. With N_b unlimited (as would be the case with two rings) all parameters are the same for one or two rings (at least according to the formulas in this paper).

2.7 One Ring or Two Rings?

With one ring, the maximum number of bunches is limited to approximately ≤ 200 . (I have not studied crossing angle schemes which may permit this number to be increased.) For $N_b > 200$ the luminosity \mathcal{L} has to be de-rated accordingly; $\mathcal{L} \rightarrow \mathcal{L}_{\text{actual}} = \mathcal{L} \times 200/N_b$. This correction is applied in Table 8. This table, whose entries are simply drawn from Table 6, makes it easy to choose between one and two rings. Entries in this table have been copied into the earlier Table 4. When the optimal number of bunches is less than (roughly) 200, single ring operation is satisfactory, and hence favored. When the optimal number of bunches is much greater than 200, for example at the Z_0 energy, two rings are better.

Note though, that the Z_0 single ring luminosities are still very healthy. In fact, with $\beta_y^*=10$ mm, which is a more conservative estimate than most others in this paper and in other FCC reports, the Z_0 single ring penalty is substantially less.

Luminosities and optimal numbers of bunches in a second generation scaled-up-luminosity Higgs factory running are shown in Figure 6.

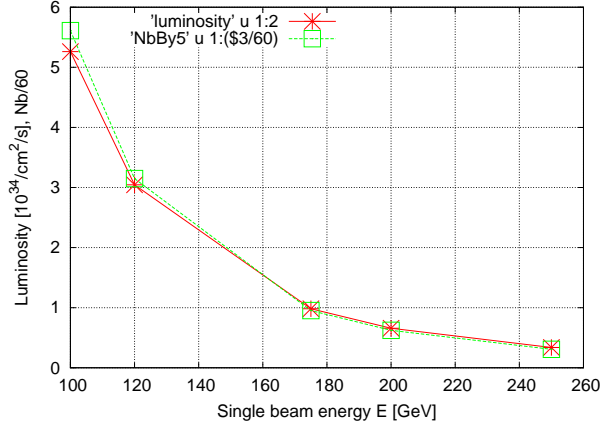


Figure 6: Dependence of luminosity on single beam energy (after upgrade to Stage II luminosity). The number of bunches (axis label to be read as $N_b/60$) is also shown, confirming that (as long as the optimal value of N_b is 1 or greater) the luminosity is proportional to the number of bunches. There is useful luminosity up to $E = 500$ GeV CM energy.

2.8 Predicted Luminosities

With one 100 km circumference ring, the maximum number of bunches is limited to about 200. For $N_b < 200$ the luminosity \mathcal{L} has to be reduced proportionally. $\mathcal{L} \rightarrow \mathcal{L}_{\text{actual}} = \mathcal{L} \times N_b/200$. Luminosities in the 100 km, 25 MW case are given in Section “Ring Circumference and Two Rings vs One Ring”. Here, for comparison, and to more nearly match the separation scheme shown in Figure 11, the circumference is assumed to be $C=50$ km, the RF power 50 MW per beam, and the number of bunches $N_b=112$. The results are shown in Table 7 (unlimited N_b) and Table 9 (with $N_b=112$).

The values of parameters not shown in the tables are $\eta_{\text{TelNov}}=0.01$, $\beta_y^*=5$ mm, $x_i^{\text{LYP}}/\beta_y^*=22.8$, $\tau_{\text{bs}}=600$ s, Optimistic= 1.5, $R_{\text{Gau-unif}}=0.30$, $eV_{\text{rf}}=20$ GeV, $OV_{\text{req.}}=20$ GV, $a_{xy}=15$, $r_{yz}=1$, $\beta_{x,\text{arcmax}}=120$ m.

2.9 Reconciling the Luminosity Formulas

Several formulas have been given for the luminosity. The luminosity actually predicted is the smallest of the entries in the three luminosity columns, for example in Table 6. For the middle shaded row the lowest value is $\mathcal{L} = 1.14 \times 10^{34} \text{ cm}^{-2}\text{s}^{-1}$.

Including some formulas already given, the following sequence of equations supports a strategy for searching param-

Parameter	Symbol	Value	Unit	Energy-scaled	Radius-	scaled
bend radius	R	3026	m	3026	5675	11350
	$R/3026$			1	1.875	3.751
Beam Energy	E	45.6/91.5	GeV	120	120	120
Circumference	C	26.66	km	26.66	50	100
Cell length	L_c		m	79	108	153
Momentum compaction	α_c	1.85e-4		1.85e-4	0.99e-4	0.49e-4
Tunes	Q_x	90.26		90.26	123.26	174.26
	Q_y	76.19		76.19	104.19	147.19
Partition numbers	$J_x/J_y/J_e$	1/1/2		1/1.6/1.4 !	1/1/2	1/1/2
Main bend field	B_0	0.05/0.101	T	0.1316	0.0702	0.0351
Energy loss per turn	U_0	0.134/2.05	GeV	6.49	3.46	1.73
Radial damping time	τ_x	0.06/0.005	s	0.0033	0.0061	0.0124
	τ_x/T_0	679/56	turns	37	69	139
Fractional energy spread	σ_δ	0.946e-3/1.72e-3		0.0025	0.0018	0.0013
Emittances (no BB), x	ϵ_x	22.5/30	nm	21.1	8.2	2.9
y	ϵ_y	0.29/0.26	nm	1.0	0.4	0.14
Max. arc beta functs	β_x^{\max}	125	m	125	171	242
Max. arc dispersion	D^{\max}	0.5	m	0.5	0.5	0.5
Beta functions at IP	β_x^*, β_y^*	2.0, 0.05	m	1.25/0.04	N/Sc.	N/Sc.
Beam sizes at IP	σ_x^*, σ_y^*	211, 3.8	μm	178/11	N/Sc.	N/Sc.
Beam-beam parameters	ξ_x, ξ_y	0.037, 0.042		0.06/0.083	N/Sc.	N/Sc.
Number of bunches	N_b	8		4	N/Sc.	N/Sc.
Luminosity	\mathcal{L}	2e31	$\text{cm}^{-2}\text{s}^{-1}$	1.0e32	N/Sc.	N/Sc.
Peak RF voltage	V_{RF}	380	MV	3500	N/Sc.	N/Sc.
Synchrotron tune	Q_s	0.085/0.107		0.15	N/Sc.	N/Sc.
Low curr. bunch length	σ_z	0.88	cm	$\frac{\alpha_c R \sigma_e}{Q_s E}$	N/Sc.	N/Sc.

Table 5: Higgs factory parameter values for 50 km and 100 km options. The entries are mainly extrapolated from Jowett’s, 45.6 GeV report [8], and educated guesses. “N/Sc.” indicates (important) parameters too complicated to be estimated by scaling. Duplicate entries in the third column, such as 45.6/91.5 are from Jowett [8]; subsequent scalings are based on the 45.6 GeV values.

eter space for the optimal design.

$$\mathcal{L}_{\text{pow}}^{\text{RF}} = \frac{N^*}{N_b} H(r_{yz}) \frac{1}{a_{xy}} \frac{f}{4\pi} \left(\frac{n_1 P_{\text{rf}} [\text{MW}]}{\sigma_y} \right)^2, \quad (14)$$

$$N_{\text{tot}} = n_1 P_{\text{rf}} [\text{MW}], \quad (15)$$

$$A_{\beta_y} = \pi \sigma_x \sigma_y = \frac{N_p r_e}{2\gamma} \frac{1}{(\xi^{\text{sat.}}/\beta_y)} = \pi \sigma_x \sigma_y, \quad (16)$$

$$\mathcal{L}_{\text{sat}}^{\text{bb}} = N^* N_b N_p H(r_{yz}) f \frac{\gamma}{2r_e} (\xi^{\text{sat.}}/\beta_y), \quad (17)$$

$$\mathcal{L}_{\text{trans}}^{\text{bs}} = N^* N_b H(r_{yz}) a_{xy} \sigma_z^2 f \left(\frac{\sqrt{\pi} 1.96 \times 10^5}{28.0 \text{ m } \sqrt{2/\pi}} \right)^2 \times \frac{1}{r_e^2 \tilde{E}^2} \left(\frac{91\eta}{f n_{y,1}^* \mathcal{R}_{\text{Gauss}}^{\text{unif.}}} \right)^2, \quad (18)$$

$$N_b = \sqrt{\frac{\mathcal{L}_{\text{sat}}^{\text{bb}}}{\mathcal{L}_{\text{trans}}^{\text{bs}}}}. \quad (19)$$

Under ideal single beam conditions, the beam height σ_y is vanishingly small and Eq. (14) predicts infinite luminosity, even for arbitrarily small RF power. Of course this is nonsense; nature “abhors” both zero and infinity. In fact, when in collision, the beam-beam force causes σ_y to grow (as the simulation model assumes). In the current context this implies that it is *always* possible to saturate the tune shift op-

erationally. In this circumstance Eq. (16) is applicable, and gives the beam area A_{β_y} , small enough for the tune shift to be saturated with the available number of electrons, which is given by Eq. (16). Tentatively we assume $N_b = 1$ and, therefore, $N_p = N_{\text{tot}}$. Then

$$\sigma_y = \sqrt{\frac{A_{\beta_y}}{\pi a_{xy}}}, \quad \text{and} \quad \sigma_x = a_{xy} \sigma_y. \quad (20)$$

With the beam aspect ratio a_{xy} being treated as if known, this permits the bunch height and width to be determined. But this determination is only preliminary since the number of bunches N_b is not yet fixed. Then, for a tentatively adopted value of bunch length σ_z , with $(\xi^{\text{sat.}}/\beta_y)$ read from Figure 5, Eq. (17) gives the predicted luminosity with all the beam in one bunch.

But this has neglected the beamstrahlung limitation; Eq. (18) gives the maximum luminosity allowed by beamstrahlung. (Factors have not been collected in this embarrassingly-cluttered formula so they can be traced from earlier formulas.) This beamstrahlung-limited luminosity will usually be less than the beam-power limited luminosity. The only recourse in this case is to split the beam into N_b bunches. Changing N_b does not change $\mathcal{L}_{\text{sat}}^{\text{bb}}$, because $N_b N_p$ is fixed, but it increases $\mathcal{L}_{\text{trans}}^{\text{bs}}$, and it decreases

name	E GeV	ϵ_x nm	β_y^* mm	ϵ_y pm	ξ_{sat}	N_{tot} 10^{12}	σ_y μm	σ_x μm	u_c^* GeV	$n_{\gamma,1}^*$	\mathcal{L}^{RF} 10^{34}	$\mathcal{L}_{\text{trans}}^{\text{bs}}$ 10^{34}	\mathcal{L}^{bb} 10^{34}	N_b	β_x^* m	P_{rf} MW
Z	46	0.949	2	63.3	0.094	1500	0.356	5.34	0.000	2.01	52.5	103	52.5	65243	0.03	25
W	80	0.336	2	22.4	0.101	150	0.212	3.17	0.001	2.10	9.66	17.2	9.6	10980	0.03	25
LEP	100	0.223	2	14.9	0.101	62	0.172	2.59	0.002	2.13	4.95	8.46	4.94	5421	0.03	25
H	120	0.159	2	10.6	0.102	30	0.146	2.19	0.003	2.17	2.86	4.74	2.86	3044	0.03	25
tt	175	0.078	2	5.33	0.118	6.6	0.103	1.55	0.006	2.24	0.923	1.43	0.92	920	0.03	25
Z	46	17.2	5	1140	0.094	1500	2.39	35.89	0.001	2.16	21	35.1	21	3605	0.075	25
W	80	6.11	5	408	0.101	150	1.43	21.42	0.003	2.26	3.86	5.83	3.86	602	0.075	25
LEP	100	4.07	5	271	0.101	62	1.16	17.47	0.005	2.31	1.98	2.86	1.97	296	0.075	25
H	120	2.92	5	195	0.102	30	0.987	14.80	0.008	2.35	1.15	1.6	1.14	166	0.075	25
tt	175	1.47	5	98.1	0.118	6.6	0.7	10.51	0.017	2.43	0.369	0.479	0.37	49	0.075	25
Z	46	155	10	10300	0.094	1500	10.2	152.3	0.002	2.29	10.5	15.5	10.5	400	0.15	25
W	80	55.4	10	3690	0.101	150	6.08	91.17	0.007	2.41	1.93	2.55	1.93	66	0.15	25
LEP	100	37.0	10	2470	0.101	62	4.97	74.48	0.011	2.46	0.989	1.25	0.99	32	0.15	25
H	120	26.6	10	1770	0.102	30	4.21	63.15	0.016	2.50	0.573	0.696	0.57	18.3	0.15	25
tt	175	13.5	10	898	0.118	6.6	3.0	44.94	0.036	2.60	0.185	0.207	0.19	5.5	0.15	25

Table 6: The major factors influencing luminosity, assuming 100 km circumference and 25 MW/beam RF power. The predicted luminosity is the smallest of the three luminosities, \mathcal{L}^{RF} , $\mathcal{L}_{\text{trans}}^{\text{bs}}$, and \mathcal{L}^{bb} . All entries in this table apply to either one ring or two rings, except where the number of bunches N_b is too great for a single ring.

name	E GeV	ϵ_x nm	β_y^* mm	ϵ_y pm	ξ_{sat}	N_{tot}	σ_y μm	σ_x μm	u_c^* GeV	$n_{\gamma,1}^*$	\mathcal{L}^{RF} 10^{34}	$\mathcal{L}_{\text{trans}}^{\text{bs}}$ 10^{34}	\mathcal{L}^{bb} 10^{34}	N_b	β_x^* m	P_{rf} MW
Z	46	0.916	2	61.1	0.094	7.3e+14	0.35	5.24	0.000	1.97	52.5	96.8	52.513	33795	0.03	50
W	80	0.323	2	21.6	0.101	7.6e+13	0.208	3.12	0.001	2.06	9.66	16.2	9.661	5696	0.03	50
LEP	100	0.215	2	14.3	0.101	3.1e+13	0.169	2.54	0.002	2.10	4.95	8	4.947	2814	0.03	50
H	120	0.153	2	10.2	0.102	1.5e+13	0.143	2.15	0.003	2.13	2.86	4.48	2.863	1581	0.03	50
tt	175	0.077	2	5.12	0.118	3.3e+12	0.101	1.52	0.006	2.19	0.923	1.35	0.923	478	0.03	50
Z	46	16.5	5	1100	0.094	7.3e+14	2.35	35.21	0.001	2.12	21	33.2	21.005	1872	0.075	50
W	80	5.88	5	392	0.101	7.6e+13	1.4	20.99	0.003	2.22	3.86	5.52	3.864	313	0.075	50
LEP	100	3.91	5	261	0.101	3.1e+13	1.14	17.12	0.005	2.26	1.98	2.71	1.979	154	0.075	50
H	120	2.80	5	187	0.102	1.5e+13	0.966	14.50	0.007	2.30	1.15	1.52	1.145	86	0.075	50
tt	175	1.41	5	94	0.118	3.3e+12	0.686	10.28	0.016	2.38	0.369	0.455	0.369	26	0.075	50
Z	46	149	10	9900	0.094	7.3e+14	9.95	149.28	0.002	2.24	10.5	14.7	10.503	208	0.15	50
W	80	53.1	10	3540	0.101	7.6e+13	5.95	89.26	0.007	2.36	1.93	2.42	1.932	34	0.15	50
LEP	100	35.4	10	2360	0.101	3.1e+13	4.86	72.88	0.011	2.41	0.989	1.19	0.989	17	0.15	50
H	120	25.4	10	1700	0.102	1.5e+13	4.12	61.78	0.016	2.45	0.573	0.663	0.573	9.5	0.15	50
tt	175	12.9	10	857	0.118	3.3e+12	2.93	43.92	0.035	2.54	0.185	0.198	0.185	2.9	0.15	50

Table 7: Luminosity influencing parameters and luminosities with unlimited number of bunches N_b , assuming 50 km circumference ring and 50 MW per beam RF power.

E GeV	β_y^* m	ξ_{sat}	$\mathcal{L}^{\text{actual}}$ 10^{34}	$N_{b,\text{actual}}$	P_{rf} MW/beam
46	0.002	0.094	0.161	200	25
80	0.002	0.1	0.176	200	25
100	0.002	0.1	0.182	200	25
120	0.002	0.1	0.188	200	25
175	0.002	0.12	0.200	200	25
46	0.005	0.094	1.165	200	25
80	0.005	0.1	1.282	200	25
100	0.005	0.1	1.334	200	25
120	0.005	0.1	1.145	166	25
175	0.005	0.12	0.369	50	25
46	0.010	0.094	5.247	200	25
80	0.010	0.1	1.932	66.5	25
100	0.010	0.1	0.989	32.7	25
120	0.010	0.1	0.573	18.3	25
175	0.010	0.12	0.185	5.5	25

Table 8: Luminosities achievable with a single ring for which the number of bunches N_b is limited to 200, assuming 100 km circumference and 25 MW/beam RF power. Entries in this table have been distilled down to include only the most important entries in Table 6, as corrected for the restricted number of bunches. The luminosity entries in Table 4 have been obtained from this table.

E GeV	β_y^* m	ξ_{sat}	$\mathcal{L}^{\text{actual}}$ 10^{34}	$N_{b,\text{actual}}$	P_{rf} MW
46	0.002	0.094	0.174	112	50
80	0.002	0.1	0.190	112	50
100	0.002	0.1	0.197	112	50
120	0.002	0.1	0.203	112	50
175	0.002	0.12	0.216	112	50
46	0.005	0.094	1.256	112	50
80	0.005	0.1	1.380	112	50
100	0.005	0.1	1.434	112	50
120	0.005	0.1	1.145	86.6	50
175	0.005	0.12	0.369	26.1	50
46	0.010	0.094	5.644	112.0	50
80	0.010	0.1	1.932	34.7	50
100	0.010	0.1	0.989	17.1	50
120	0.010	0.1	0.573	9.5	50
175	0.010	0.12	0.185	2.9	50

Table 9: Luminosity influencing parameters and luminosities with the number of bunches limited to $N_b = 112$, assuming 50 km circumference ring and 50 MW per beam RF power.

$\mathcal{L}_{\text{pow}}^{\text{RF}}$ by the same factor. Unfortunately, not yet definitively knowing σ_y , we cannot yet reckon the optimal value of N_b .

As a compromise we use the square-rooted ratio in Eq. (19) to fix N_b . This increases $\mathcal{L}_{\text{trans}}^{\text{bs}}$ and decreases $\mathcal{L}_{\text{pow}}^{\text{RF}}$ by the same factor (assuming $N_b > 1$).

A more aggressive approach is to replace Eq. (19) by $N_b = \mathcal{L}_{\text{sat}}^{\text{bb}} / \mathcal{L}_{\text{trans}}^{\text{bs}}$. This is justifiable, since $\mathcal{L}_{\text{sat}}^{\text{bb}}$ depends

4 LATTICE OPTIMIZATION FOR TOP-OFF INJECTION

This section discusses Higgs factory injection. Full energy, top-off injection is assumed. Vertical injection seems preferable to horizontal (as will be shown). Kicker-free, bunch-by-bunch injection concurrent with physics running may be feasible. Achieving high efficiency injection justifies optimizing injector and/or collider lattices for maximum injection efficiency. Stronger focusing in the injector and weaker focusing in the collider improves the injection efficiency. Scaling formulas (for the dependence on ring radius R) show injection efficiency increasing with increasing ring circumference. Scaling up from LEP, more nearly optimal parameters for both injector and collider are obtained. Maximum luminosity adjusting the collider cell length L_c for maximum luminosity and choosing

a shorter injector cell length, $L_i < L_c$, for maximizing injection efficiency.

4.1 Injection Strategy: Strong Focusing Injector, Weak Focusing Collider

Introduction. I take it as given that full energy top-off injection will be required for the FCC electron-positron Higgs factory. Without reviewing the advantages of top-off injection, one has to be aware of one disadvantage. The cost in energy of losing a full energy particle due to injection inefficiency is the same as the cost of losing a circulating particle to Bhabha scattering or to beamstrahlung or to any other loss mechanism. Injection efficiency of 50% is equivalent to doubling the irreducible circulating beam loss rate. To make this degradation unimportant one should therefore try to achieve 90% injection efficiency.

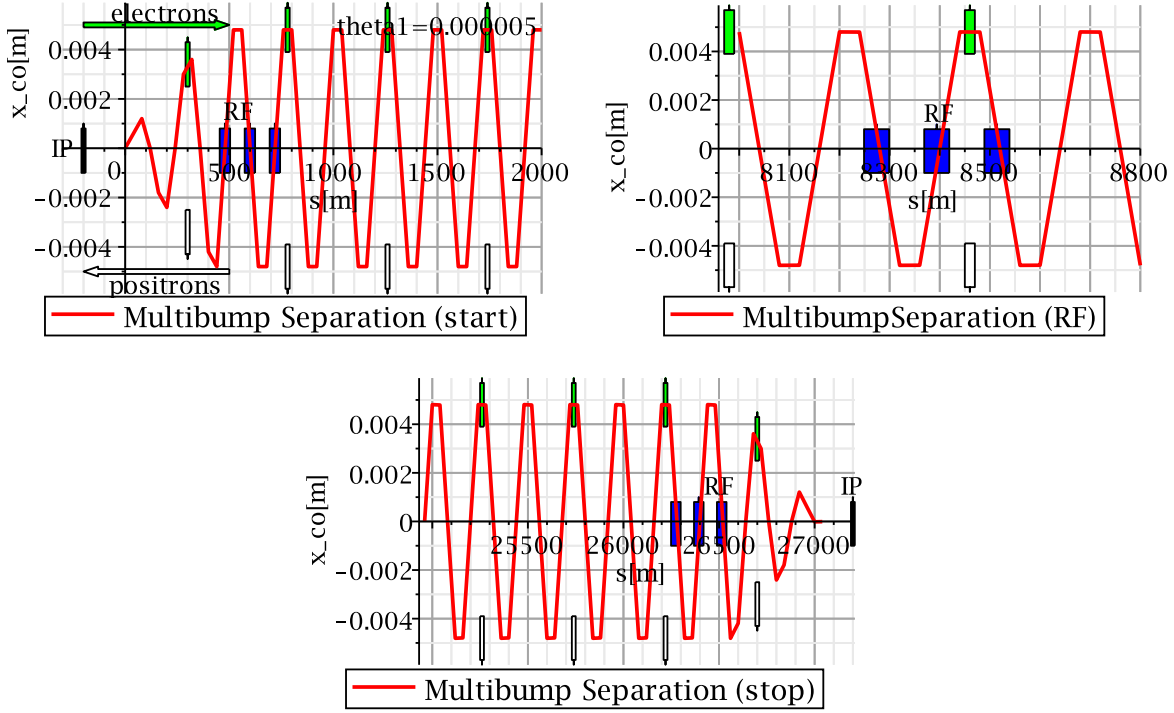


Figure 11: Short partial sections of the multibump beam separation are shown: one at the beginning, one at an RF location in the interior, and one at the far end of a long arc in Figure 8. The bunch separations are 480 m in a 50 km ring with cell length $L_c = 60$ m. IP's are indicated by vertical black bars, RF cavities by blue rectangles, electron bunches are green rectangles moving left to right, positron bunches are open rectangles moving from right to left. Counter-circulating bunches are separated at closed bump loop locations, and they must not pass through the nodes at the same time.

Achieving high efficiency injection is therefore sufficiently important to justify optimizing one or both of injector and collider lattices to improve injection. The aspect of this optimization to be emphasized here is shrinking the injector beam emittances and expanding the collider beam acceptances by using stronger focusing in the injector than in the collider. What are the dynamic aperture implications? They will be shown to be progressively more favorable as the ring radius R is increased relative to the LEP value. The dynamic-aperture/beam-width ratio increases as $R^{1/2}$ and is the same for injector and collider.

4.2 Constant Dispersion Scaling with R

Linear Lattice Optics. Most of the following scaling formulas come from Jowett [8] or Keil [10] or from reference [11]. The emphasis on parameter scaling is in very much the spirit emphasized by Alex Chao [12]. For simplicity, even if it is not necessarily optimal, assume the Higgs factory arc optics can be scaled directly from LEP values, which are: phase advance per cell $\mu_x = \pi/2$, full cell length $L_c = 79$ m. (The subscript “c” distinguishes the collider lattice cell length from the injector lattice cell length L_i .) At constant phase advance, the beta function β_x scales as L_c and dispersion D scales as bend angle per cell $\phi = L_c/R$ multiplied by cell length L_c ;

$$D \propto \frac{L_c^2}{R}. \quad (24)$$

(For 90 degree cells, the constant of proportionality in this formula is approximately 0.5, for the average dispersion $\langle D \rangle$.) Holding L_c constant as R is increased would decrease the dispersion, impairing our ability to control chromaticity. Let us therefore *tentatively adopt the scaling*

$$L_c \propto R^{1/2}, \quad \text{corresponding to } \phi \propto R^{-1/2}. \quad (25)$$

This is tantamount to holding dispersion D constant, and is consistent with electron storage ring design trends over the decades.

These quantities and “Sands curly H” \mathcal{H} then scale as

$$\beta_x \propto R^{1/2}, \quad D \propto 1, \quad \mathcal{H} \propto \frac{D^2}{\beta_x} \propto \frac{1}{R^{1/2}}. \quad (26)$$

Copied from Jowett [8], the fractional energy spread is given by

$$\sigma_\epsilon^2 = \frac{55}{32\sqrt{3}} \frac{\hbar}{m_e c} \gamma_e F_\epsilon, \quad \text{where}$$

$$F_\epsilon = \frac{\langle 1/R^3 \rangle}{J_x \langle 1/R^2 \rangle} \propto \frac{1}{R}, \quad (27)$$

and the horizontal emittance is given by

$$\epsilon_x = \frac{55}{32\sqrt{3}} \frac{\hbar}{m_e c} \gamma_e F_x, \quad \text{where}$$

$$F_x = \frac{\langle \mathcal{H}/R^3 \rangle}{J_x \langle 1/R^2 \rangle} \propto \frac{1}{R^{3/2}}. \quad (28)$$

The betatron contribution to beam width scales as

$$\sigma_{x,\text{betatron}} \propto \sqrt{\beta_x \epsilon_x} \propto 1/R^{1/2}. \quad (29)$$

Similarly, at fixed beam energy, the fractional beam energy (or momentum) spread σ_δ scales as

$$\sigma_\delta \propto \sqrt{B} \propto 1/R^{1/2}. \quad (30)$$

Scaling with R of Arc Sextupole Strengths and Dynamic Aperture. At this stage in the Higgs Factory design, it remains uncertain whether the IP-induced chromaticity can be cancelled locally, which promises more than a factor of two increase in luminosity, but would require strong bends close to the IP. For the time being I assume the IP chromaticity is cancelled in the arcs. Individual sextupole strengths can be apportioned as

$$S = S^{\text{arc chr.}} + S^{\text{IP chr.}} \quad (31)$$

The IP-compensating sextupole portion $S^{\text{IP chr.}}$ depends on the IP-induced chromaticity. A convenient rule of thumb has the IP chromaticity equal to the arc chromaticity. By this rule doubling the arc-compensating sextupole strengths cancels both the arc and the IP chromaticity.

With dispersion $D \propto 1$, quad strength $q \propto 1/R^{1/2}$, and $S^{\text{arc chr.}} \propto q/D$, one obtains the scaling of sextupole strengths and dynamic aperture;

$$S \propto \frac{1}{R^{1/2}}, \quad \text{and} \quad x^{\text{dyn. ap.}} \propto \frac{q}{S^{\text{arc chr.}}} \propto 1. \quad (32)$$

The most appropriate measure of dynamic aperture is its ratio to beam width,

$$\frac{x^{\text{dyn. ap.}}}{\sigma_x} \propto \frac{1}{1/R^{1/2}} \propto R^{1/2}. \quad (33)$$

The increase of this ratio with increasing R would allow the IP optics to be more aggressive for the Higgs factory than for LEP. Unfortunately it is the chromatic mismatch between IP and arc that is thought to be more important in limiting the dynamic aperture than is the simple compensation of total chromaticity. The constant dispersion scaling formulas derived so far are given in Table 3.

4.3 Revising Injector and/or Collider Parameters for Improved Injection

What has been discussed so far has been ‘‘constant dispersion scalling’’. But, as already stated, we wish to differentiate the injector and collider optics such that the injector emittances are smaller and the collider acceptances are larger. This can be accomplished by shortening injector length L_i and lengthening collider cell length L_c . The resulting R -dependencies and scaling formulas are shown in Table 10. They yield the lattice parameters in Table 11 for both the 50 km and 100 km circumference options.

Implications of Changing Lattices for Improved Injection. According to these calculations there is substantial advantage and little disadvantage to strengthening the injector focusing and weakening the collider focusing. This is achieved by shortening the injector cell length L_i and increasing the collider cell length L_c . Weakening the collider focusing has the effect of increasing the equilibrium transverse beam dimensions.

As indicated in the caption to Table 11, the improvement in the injector emittance/collider acceptance ratio is probably unnecessarily large, at least for a 100 km ring, where the improvement in the injector/collider emittance ratio is a factor of seven.

Furthermore there is at least one more constraint that needs to be met. Maximum luminosity results only when the beam aspect ratio at the crossing point is optimal. Among other things this imposes a condition of the horizontal emittance ϵ_x . At the moment the preferred method for controlling ϵ_x is by the appropriate choice of cell length L_c . With lattice manipulations other than changing the cell length it may be possible to increase, but probably not decrease ϵ_x .

According to Table 2 of Section ‘‘Ring Circumference and Two Rings vs One Ring’’, with $\beta_y^* = 5$ mm the optimal choice of ϵ_x is 3.98 nm. According to Table 11 the actual value will be $\epsilon_x = 7.82$ nm. These values can be considered ‘‘close enough for now’’, or they can be considered different enough to argue that further design refinement is required (which is obvious in any case). But the suggestion is that the $L_c = 213$ m collider cell length choice in Table 11 may be somewhat too long.

Unfortunately the optimal value of ϵ_x depends strongly on the optimal value of β_y^* , which is presently unknown. These considerations show that the arc and intersection region designs cannot be separately optimized. Rather a full ring optimization is required.

Parameter	Symbol	Proportionality	$L \propto R^{1/4}$ injector	$L \propto R^{1/2}$	$L \propto R^{3/4}$ collider
phase advance per cell	μ_x		90°	90°	90°
cell length	L		$R^{1/4}$	$R^{1/2}$	$R^{3/4}$
			110 m	153 m	213 m
bend angle per cell	ϕ	$= L/R$	$R^{-3/4}$	$R^{-1/2}$	$R^{-1/4}$
momentum compaction		ϕ^2	$R^{-3/2}$	R^{-1}	$R^{-1/2}$
quad strength (1/f)	q	1/L	$R^{-1/4}$	$R^{-1/2}$	$R^{-3/4}$
dispersion	D	ϕL	$R^{-1/2}$	1	$R^{1/2}$
beta	β	L	$R^{1/4}$	$R^{1/2}$	$R^{3/4}$
tune	Q_x	R/β	$R^{3/4}$	$R^{1/2}$	$R^{1/4}$
			243.26	174.26	125.26
tune	Q_y	R/β	$R^{3/4}$	$R^{1/2}$	$R^{1/4}$
			205.19	147.19	106.19
Sands's "curly H"	\mathcal{H}	$= D^2/\beta$	$R^{-5/4}$	$R^{-1/2}$	$R^{1/4}$
partition numbers	$J_x/J_y/J_\epsilon$	1/1/2	1/1/2	1/1/2	1/1/2
horizontal emittance	ϵ_x	$\mathcal{H}/(J_x R)$	$R^{-9/4}$	$R^{-3/2}$	$R^{-3/4}$
fract. momentum spread	σ_δ	\sqrt{B}	$R^{-1/2}$	$R^{-1/2}$	$R^{-1/2}$
arc beam width-betatron	$\sigma_{x,\beta}$	$= \sqrt{\beta\epsilon_x}$	R^{-1}	$R^{-1/2}$	1
-synchrotron	$\sigma_{x,synch.}$	$= D\sigma_\delta$	R^{-1}	$R^{-1/2}$	1
sextupole strength	S	q/D	$R^{1/4}$	$R^{-1/2}$	$R^{-5/4}$
dynamic aperture	x^{da}	q/S	$R^{-1/2}$	1	$R^{1/2}$
relative dyn. aperture	x^{da}/σ_x		$R^{1/2}$	$R^{1/2}$	$R^{1/2}$
separation amplitude	x_p	σ_x	N/A	$R^{-1/2}$	1

Table 10: To improve injection efficiency (compared to constant dispersion scaling) the injector cell length can increase less, for example $L_i \propto R^{1/4}$, and the collider cell length can increase more, for example $L_i \propto R^{3/4}$. The shaded entries assume circumference $C=100$ km, $R/R_{LEP}=3.75$.

Parameter	Symbol	LEP(sc)	Unit	Injector		Collider	
bend radius	R	3026	m	5675	11350	5675	11350
beam Energy		120	GeV	120	120	120	120
circumference	C	26.7	km	50	100	50	100
cell length	L	79	m	92.4	110	127	213
momentum compaction	α_c	1.85e-4	m	0.72e-4	0.25e-4	1.35e-4	0.96e-4
tunes	Q_x	90.26		144.26	243.26	105.26	125.26
	Q_y	76.19		122.19	205.19	89.19	106.19
partition numbers	$J_x/J_y/J_\epsilon$	1/1.6/1.4		1/1/2	1/1/2	1/1/2	1/1/2
main bend field	B_0	0.1316	T	0.0702	0.0351	0.0702	0.0351
energy loss per turn	U_0	6.49	GeV	3.46	1.73	3.46	1.73
radial damping time	τ_x	0.0033	s	0.0061	0.0124	0.0061	0.0124
	τ_x/T_0	37	turns	69	139	69	139
fractional energy spread	σ_δ	0.0025		0.0018	0.0013	0.0018	0.0013
emittances (no BB), x	ϵ_x	21.1	nm	5.13	1.08	13.2	7.82
y	ϵ_y	1.0	nm	0.25	0.05	0.66	0.39
max. arc beta functs	β_x^{\max}	125	m	146	174	200	337
max. arc dispersion	D^{\max}	0.5	m	0.37	0.26	0.68	0.97
quadrupole strength	$q \approx \pm 2.5/L_p$	0.0316	1/m	0.027	0.0227	0.0197	0.0117
max. beam width (arc)	$\sigma_x = \sqrt{2\beta_x^{\max}\epsilon_x}$	$1.6\sqrt{2}$	mm	$0.865\sqrt{2}$	$0.433\sqrt{2}$	$1.62\sqrt{2}$	$1.62\sqrt{2}$
(ref) sextupole strength	$S = q/D$	0.0632	1/m ²	0.0732	0.0873	0.0290	0.0121
(ref) dynamic aperture	$x^{da} \sim q/S$	~ 0.5	m	~ 0.370	~ 0.260	~ 0.679	~ 0.967
(rel-ref) dyn.ap.	x^{da}/σ_x	~ 0.313		~ 0.428	~ 0.600	~ 0.417	~ 0.621
separation amplitude	$\pm 5\sigma_x$	$\pm 8.0\sqrt{2}$	mm			$\pm 8.1\sqrt{2}$	$\pm 7.8\sqrt{2}$

Table 11: Lattice parameters for improved injection efficiency. This table is to be compared with Table 5 to assess the effect of lattice changes on injection efficiency. The shaded row indicates how successfully the injector emittance has been reduced relative to the collider emittance. The factor of seven improvement, 7.82/1.08, in this ratio for a 100 km ring, seems unnecessarily large, indicating that less radical scaling should be satisfactory.

5 $\mathcal{L} \times L^{*2}$ LUMINOSITY \times FREE SPACE INVARIANT

Yunhai Cai's intersection region design [13] is analysed in detail in Appendix E, "Deconstructing Yunhai Cai's IR Optics". For maximum operational convenience in changing IP beta functions, Yunhai's design was designed to be scalable. This makes the IR design ideal for using dimensional analysis to derive scaling law dependence on the free space length L^* , which is the length of the space left free for the particle collision reconstruction apparatus. This scaling law can be employed to investigate how the choice of free IP length L^* affects the achievable luminosity. Yunhai's design is probably close to optimal. But, even if it is not, the same results, based purely on scaling behavior, will still be valid. This prescription does not establish the absolute luminosity but it does determine the relative luminosity under the plausible hypothesis that the luminosity maximum will be governed by the maximum β functions. (anywhere in the ring). Following the derivation of this scaling law its impact on operations will be discussed.

MAD runs produced the beta function plots shown in Figure 12 for the four parameter sets given in Table 12. Other than noting their identical shapes (confirming the scaling) only the maximum β_y^{\max} values are extracted from the plots.

Results of the MAD runs are plotted in Figure 13. The smooth fitting function in the left plot of Figure 13 gives the scaling law

$$\beta_y^{\max} = \frac{10[\text{m}^2]}{\beta_y^*} \left(\frac{L^*}{L^{*\text{nom}}} \right)^p, \quad (34)$$

where $L^{*\text{nom}} = 2 \text{ m}$ is the nominal distance from IP to the entrance edge of the first quadrupole. The final factor (which is equal to 1 for the plot) has been included to allow power law dependence on L^* , with exponent p to be determined later. The right plot of Figure 13 gives the scaling law

$$\beta_y^* = \beta_y^{*\text{nom}} \left(\frac{L^*}{L^{*\text{nom}}} \right)^2. \quad (35)$$

Re-arranging Eq. (34) gives

$$\beta_y^* = \frac{10[\text{m}^2]}{\beta_y^{\max}} \left(\frac{L^*}{L^{*\text{nom}}} \right)^p. \quad (36)$$

For Eqs. (35) and (36) to be compatible requires $p = 2$. Then Eq. (36) becomes

$$\beta_y^* = 2.5 \frac{L^{*2}}{\beta_y^{\max}} \stackrel{\text{e.g.}}{=} 2.5 \frac{2^2}{4900} = 2 \text{ mm}. \quad \checkmark \quad (37)$$

Using Eq. (37) the luminosity is given by

$$\mathcal{L}^{\text{static}} = \frac{4 \times 10^{31} \text{ cm}^{-2} \text{ s}^{-1} \text{ m}}{\beta_y^*} \quad (38)$$

or

$$\mathcal{L}^{\text{static}} = 1.6 \times 10^{31} \text{ cm}^{-2} \text{ s}^{-1} \text{ m} \times \frac{\beta_y^{\max}}{L^{*2}}. \quad (39)$$

The constant of proportionality in these equation has not been determined by the scaling formula. It has been chosen to match independently estimated luminosities.

5.1 Estimating β_y^{\max} (and from it \mathcal{L})

According to Eq. (39) the achievable luminosity \mathcal{L} is proportional to the maximum achievable beta function value

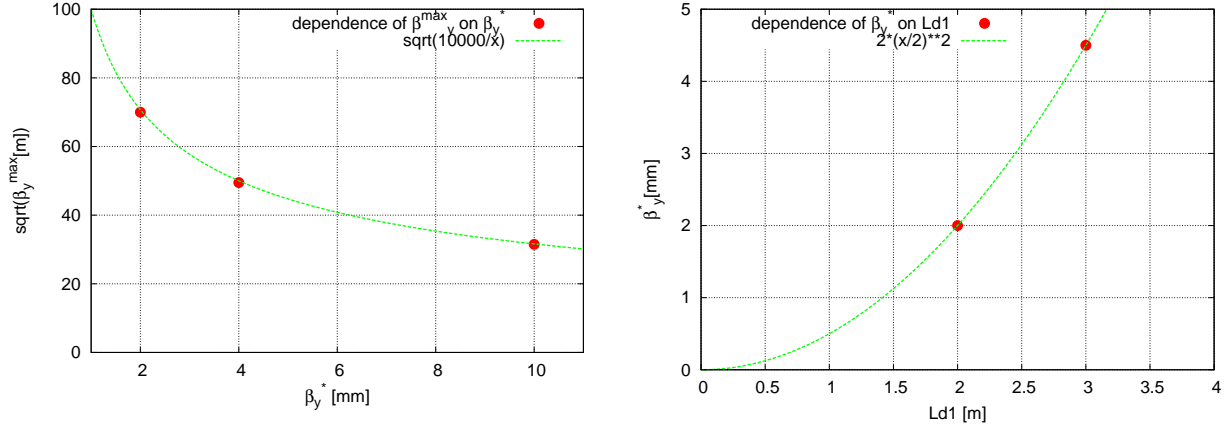


Figure 13: Parameter dependencies implied by the Yunhai Cai intersection region design. The left plots β_Y^{\max} (or rather its square root) versus β_Y^* with the longitudinal scale held constant. The right plots β_Y^* versus L^* with $\beta_Y^{\max} = 4900$ m held constant.

Using $q \propto 1/L_c$, setting these equal, and solving for Δx^{tol} .

$$\Delta x^{\text{tol}} = \frac{DL_c}{\beta_y^{\max}}. \quad (41)$$

Dimensionally this quantity is a length. It depends primarily on unknown transverse positioning imperfections. Its absolute magnitude can therefore only be inferred phenomenologically, by substituting the operationally determined value of β_y^{\max} on the right hand side.

Maximum β_y Phenomenology. For half a century it has been known that the way to get higher luminosity is to reduce β_y^* —and also that this entails increasing β_y^{\max} , which is usually what is blamed for the loss of dynamic aperture that limits the ability to reduce β_y^* . In recent years linear collider studies have produced very small β_y^* designs, that are presumed to function satisfactorily for “Final Focus”; here “final focus” means the particles “die” there.

The “advantage” a circular collider has over a linear collider is that every particle has millions of chances to collide with a particle in the other beam. Applying the term “final focus” to the IR of a circular collider is a crime against language. **The “disadvantage” of a circular collider is that a particle has to survive millions of passages through the other beam.** It is operational experience with this problem that is considered in this section.

One qualification is required. What most distinguishes a Higgs factory from a low energy ring such as a B factory is that RF power dominates the former, but not the latter. With RF power insignificant the number of bunches N_b can be very large and they can circulate in separate rings. RF power restricts N_b in a Higgs factory. This limits the dual ring advantage, and limits the applicability of B factory experience to the design of a Higgs factory. The extreme beam energy ratio, 120/5 also limits IR design possibilities (such as reducing L^* in the Super-KEK design). For these reasons

the present paper bases most of its estimates on extrapolation from LEP.

(Inverse) transverse sensitivity lengths are plotted for various accelerators in Table 13. For convenience in predicting β_y^{\max} for CepC, it is the inverse ratio $1/\Delta x^{\text{tol}} = \beta_y^{\max}/(DL_c)$ that is tabulated.

β_y^* m	Ring		D m	L_c m	DL_c m ²	β_y^{\max} m	$\frac{\beta_y^{\max}}{DL_c}$ 1/m
0.015	CESR	exp.	1.1	17	18.7	95	5.1
0.08	PETRA	exp.	0.32	14.4	4.6	225	49
	HERA	exp.	1.5	48	72	2025	28
0.05	LEP	exp.	0.8	79	63	441	7.0
0.007	KEKB	exp.	0.5	20	10	290	29
	LHC	exp.	1.6	79	126	4500	36
0.01	CepC ₁	des.	0.31	47	14.6	1225	84
0.01	CepC ₂	des.	1.03	153	158	1225	8.8
0.001	CEPC	des.	0.31	47	14.6	6000	410
0.001	FCC-ee	des.	0.10	50	5.0	9025	1805

Table 13: Lattice parameters and inverse transverse sensitivity lengths β_y^{\max}/DL_c for various e+e- colliders. The upper rows contain experimentally measured values, the lower rows contain design values. CepC₁ copies the L_c and D values from CEPC, while CepC₂ copies them from Table 5. The IR design is assumed identical for CepC₁ and CepC₂, with $\beta_y^* = 10$ mm. In principle nothing in this table depends directly on β_y^* . But, indirectly, large β_y^{\max} values are correlated with small β_y^* values.

When β_y^{\max} is large, it is always because β_y^* is small. But the value of β_y^* is irrelevant in assessing the dynamic aperture limitation caused by the large value of β_y^{\max} . So no β_y^* values are given in the table. If there were, β_y^* would tend to be “big” for the ancient rings toward the top of the table, and “small” toward the bottom. The two CepC rows assume identical IP optics with $\beta_y^* = 10$ mm. For the CepC₁ row

the ring parameters are copied from the CEPC, CDR design. For the CepC₂ row the ring parameters are copied from Table 5. For the CEPC row $\beta_y^* = 1$ mm (which accounts for its hyper-transverse-sensitivity). CEPC and FCC-ee values differ due to different dispersion and different L^* values (1.5 m for CEPC, 2.0 m for FCC-ee).

Compared in this way the transverse tolerances of KEKB and LHC are close in value, even though, as storage rings, they could scarcely be more dissimilar; KEKB is a “small” electron collider, LHC is a large proton collider. The pessimistic behavior of LEP can be blamed on the absence of top-off injection, which led to the tortuous ramping and beta squeeze operations. This limited the β_y^* to be not less than 5 cm.

This transverse sensitivity discussion has been only semi-quantitative but, at least, it is dimensionally consistent, and it provides a prescription for comparing performance of very different colliders. For the “transverse sensitivity length” to be a valid comparison gauge implicitly assumes that this length (dependent of survey and positioning precision) can be expected to be the same for accelerators of all sizes, and for both electrons and protons. The approach has been somewhat *ad hoc* however, and it depends on the validity of the scaling laws emphasized in this paper. Some length other than DL_c/β_y^{\max} might provide a more valid comparison, though it would probably disrupt the good agreement between two modern rings, KEKB and LHC, in the last column of Table 13.

5.2 Turn-On Scenarios

According to Figure 27 in Section ”Deconstructing Yunhai Cai’s IR Optics“ the maximum beta function value is $\beta_y \approx 1225$ m. Note, however, that $\beta_y^* = 10$ mm is the value of the IP beta function in Figure 22. This is ten times greater than the value $\beta_y^* = 1$ mm sometimes assumed in FCC projections. According to Formula (38) $\beta_y^* = 1$ mm would imply $\beta_y^{\max} \approx 12,250$ m, which sends the transverse sensitivity off scale.

Initially one will turn on with a conservatively large value of $\beta_y^* = 10$ mm or, at first, even higher. The luminosity in Run I will therefore be fairly low. One will expect a much higher luminosity in Run II. Luminosities under this scenario are given in Table 14, for two choices of L^* .

Run	year	β_y^{\max} m	L^* m	β_y^* mm	$\mathcal{L}^{\text{stat}}$ 10^{34}	\mathcal{L}^{dyn} 10^{34}
I	2025?	1000	2	10	0.40	0.40
			3	22	0.178	0.178
II	2027?	3000	2	3.3	1.2	> 1.2
			3	7.5	0.53	> 0.53

Table 14: Projected luminosities for conservative commissioning stages for two different values of detector free space parameter L^* .